Cytotechnology (2013) 65:749–758
DOI 10.1007/s10616-013-9558-2

ORIGINAL RESEARCH

Cell tracking and velocimetric parameters analysis as an approach to assess activity of mussel (*Mytilus edulis*) hemocytes in vitro

Damien Rioult · Jean-Marc Lebel · Frank Le Foll

Received: 23 November 2012 / Accepted: 22 March 2013 / Published online: 12 April 2013

Abstract Hemocytes constitute the key element of innate immunity in bivalves, being responsible for secretion of antimicrobial peptides and release of zymogens from the prophenoloxidase system within the hemolymph compartment, reactive oxygen species production and phagocytosis. Hemocytes are found (and collected) as cells in suspension in circulating hemolymph. Hemocytes are adherent cells as well, infiltrating tissues and migrating to infected areas. In the present study, we applied an approach based on fluorescent staining and nuclei-tracking to determine migration velocity of hemocytes from the blue mussel, *Mytilus edulis*, in culture. Freshly collected hemocytes attached to substrate and start to move spontaneously in few minutes. Two main hemocyte morphologies can be observed: small star-shaped cells which were less motile and spread granular cells with faster migrations. Cell-tracking was combined to MTT mitochondria metabolic rate measurements in order to monitor global cell population activity over 4 days of culture. A transient peak of cell activity was recorded after 24–48 h of culture, corresponding to a speed up of cell migration. Videomicroscopy and cell tracking techniques provide new tools to characterize activity of mussel immunocytes in culture. Our analysis of hemocyte migration reveals that motility is very sensitive to cell environmental factors.

Keywords Marine Invertebrate · Primary cultures · Motility · Cell-tracking · Innate Immunity · Molluscs

Electronic supplementary material The online version of this article (doi:10.1007/s10616-013-9558-2) contains supplementary material, which is available to authorized users.

D. Rioult (✉) · F. Le Foll
Laboratory of Ecotoxicology, EA 3222, FED 4116
SCALE, University of Le Havre,
76058 Le Havre Cedex, France
e-mail: drioult@free.fr; damien.rioult@univ-lehavre.fr

J.-M. Lebel
CNRS INEE, FRE3484 BioMEA Biologie des
Mollusques marins et des Ecosystèmes Associés, IBFA,
University of Caen, 14032 Caen Cedex, France

Introduction

The blue mussel *Mytilus edulis* is a bivalve belonging to Mollusca, a phylum comprising the largest number of described marine species (Ponder and Lindberg 2008). These animals, living in complex estuarine and intertidal environments, experience major fluctuations of physico-chemical parameters in coastal areas (Gauthier-Clerc et al. 2013; Malagoli et al. 2007). In addition to those abiotic stressors, mussels house a variety of endoparasites and microbial organisms (Venier et al. 2011). To control host-pathogen interactions and to respond immediately to invaders, mussels as others invertebrates, rely on innate immunity. Hemocytes found in hemolymph and infiltrating tissues, constitute a heterogeneous population of immune cells actively specialized in pleiotropic defences against pathogens (Carballal et al. 1997; Donaghy and Volety 2011;

Le Foll et al. 2010). During the inflammatory response, activated hemocytes execute several major functions of cell-mediated innate immunity, including cytotoxic production of oxygen (Costa et al. 2009; Winston et al. 1996) or nitrogen species (Novas et al. 2007), increased production of lysozymes (Li et al. 2008) and phagocytosis (Carballal et al. 1997; Garcia-Garcia et al. 2008; Le Foll et al. 2010; Malagoli et al. 2007).

To be effective in host-defense, hemocytes do not require prior exposure to antigens but can express a vast repertoire of immune-related genes, over-represented in bivalves, as revealed by recent reports on sequencing of oyster genome (Zhang et al. 2012) and analyses of mussel transcriptomes after biotic and abiotic stress challenges (Craft et al. 2010; Philipp et al. 2012; Venier et al. 2011). Despite this more precise picture of molecular diversity, identity and evolution of mussel gene products acting as non-self recognition sensors, cytokine regulators, antimicrobial peptides or apoptosis/autophagy effectors (Philipp et al. 2012; Venier et al. 2011), the overall physiology of innate immunity in *Mytilidae* remains poorly understood. In particular, whereas different types of hemocytes have been described so far (Cajaraville and Pal 1995; Friebel and Renwrantz 1995; Hine 1999; Le Foll et al. 2010; Parisi et al. 2008; Donaghy and Volety 2011), the origin, the role and the activation steps of hemocyte subpopulations are unknown. Furthermore, except for phagocytosis (Garcia-Garcia et al. 2008; Le Foll et al. 2010; Voccia et al. 1994), consensual protocols quantifying hemocyte activity or functional markers of inflammatory states are still lacking.

An early and key stage of immune response consists in hemocyte recruitment and migration to the site of infection. We have previously shown that time-lapse videomicroscopy allows investigations on dynamics of mussel hemocytes shape changes and helps to propose a functional classification of cell subtypes (Le Foll et al. 2010). In the present study, we describe a novel approach based on fluorescent staining and nuclei-tracking to determine migration velocity of hemocytes in vitro. This method was applied to follow hemocyte activity over several days of culture.

Materials and methods

Reagents

Most compounds were purchased from Sigma–Aldrich (St. Louis, MO, USA). A stock solution of polyethyleneimine (PEI) was prepared from 1 g of liquid PEI (50 % w/v in water) diluted in 10 mL sterile deionised water. Hoechst 33342 was supplied by Invitrogen (Carlsbad, CA, USA).

Hemolymph withdrawal

Adult mussels (4–5 cm shell length), *M. edulis*, were collected on the intertidal rocky shore of Yport (0°18′52″E:49°44′30″N, Seine-Maritime, France) between April and June 2012 (sea surface temperature between 10 and 13 °C). Mussels were transported to the laboratory and directly used. Typically, hemolymph was aseptically withdrawn in a BSL2 laminar flow cabinet from the posterior adductor muscle sinus by gentle aspiration with a 1 mL syringe equipped with a 22G needle. Hemocytes used in the present study were withdrawn from 132 mussels collected, without hemolymph pooling.

Hemocytes culture

Distinct cell cultures were carried out from distinct individuals. In some experiments, culture plastic substrates were coated for 2 h at room temperature with PEI diluted 1/10000 from the stock solution, washed 3 times with sterile deionised water and let to dry in the BSL2 cabinet. Volumes of crude hemolymph corresponding to 100 or 200 µL from one single individual were deposited in 35-mm culture dishes (Corning, Corning, NY, USA) or in each well of 96-well culture plates, respectively. After 30 min of sedimentation, hemolymph was removed and each well or dish were washed twice by using marine physiological saline solution (MPSS) containing (in mM): 470 NaCl, 10 KCl, 10 $CaCl_2$, 10 4-(2-hydroxyethyl)piperazine-1-ethanesulfonic acid (Hepes), 48.7 $MgSO_4$, pH 7.8, 0.2 µm filtered. The cells were covered with sterile MPSS supplemented with 2 mM L-glutamine, 100 µg mL^{-1} streptomycin, 60 µg mL^{-1} penicillin G. The cells were then maintained at 14 °C in a temperature-controlled incubator.

MTT bioassay

A MTT assay was used to determine cell number in each well. In the presence of viable cells, MTT, 3-[4,5-dimethylthiazol-2-yl]-2,5-diphenyltetrazolium bromide, is enzymatically reduced to the purple dye

formazan. The assay was performed according to the manufacturer's instructions. Briefly, hemocytes were softly placed in 96-well cell culture plates and allowed to adhere for 30 min at 14 °C. Thereafter, cells were rinced with MPSS and incubated in MPSS containing 0.2 mg mL^{-1} MTT. After 4 h at 14 °C, the MTT solution was removed and 200 μL of dimethyl sulfoxide (DMSO) was added to each well to solubilize formazan crystals. The absorbance was then measured at a wavelength of 570 nm with a 630 nm reference using a micro plate reader (Elx808; Biotek, Winooski, VT, USA).

Microscopy set-up

A culture dish was placed on the stage of a TE-2000 inverted microscope (Nikon, Champigny-sur-Marne, France) equipped for epifluorescence excitation and time-lapse imaging with a moderately-cooled high-resolution charge-coupled device (CoolSnap EZ; Photometrics, Tucson, AZ, USA). A Peltier temperature controller (PDMI-2 and TC-202A; Harvard Apparatus, Holliston, MA, USA) keeps preparation at 14 °C for extended live cell imaging. Bright field images were acquired with a 40× Hoffman modulation contrast objective (numerical aperture 0.55). For epifluorescence time-lapse imaging, the same objective was used and, to prevent bleaching or phototoxicity, a VCM-D1 shutter (Uniblitz, Vincent Associates, Rochester, NY, USA) was added in the illumination pathway to cut off the excitation light between two image recordings. Camera and shutter were controlled by using Metamorph (Molecular Device, Sunnyvale, CA, USA) as acquisition software. Coolsnap camera captured a 12-bit digital of 1,392 × 1,040 pixels grayscale images every 30 s for 30 min. 1 pixel represent a 6.45 × 6.45-μm square. Camera and software were calibrated with the 40× objective to express distance in microns.

Bight field videomicroscopy

One hundred microliter of freshly withdrawn hemolymph were placed in a 35 mm non treated polystyrene culture dish (BD Falcon Easy Grip, Becton Dickinson, Franklin Lakes, NJ, USA). Cells were allowed to adhere for 30 min at room temperature and covered by 2 mL of MPSS. The culture dish was transferred on the stage of a TE-2000 inverted microscope for time lapse imaging using the 40× Hoffmann modulation contrast objectives.

Cells tracking and analysis

To quantify velocity, cells in culture were incubated with 10 μM of the nuclei-specific fluorescent probe Hoechst 33342 for 30 min at 14 °C. Afterwards, the culture dish was transferred on the stage of the microscope to record movies. Hoffman modulation contrast optics were used to obtain cells images before and after the fluorescence imaging. Movie was imported into Metamorph Analysis software. Track Objects application (available with Multi-Dimensional Motion Analysis option) was started. Twenty nuclei were randomly chosen to be tracked. Extracted data were transferred to a spreadsheet and, for each cell, the mean distance travelled during 30 s was calculated and multiplied by 2 to express velocity in μm min^{-1}.

Statistical analysis

All quantitative data were expressed as mean ± standard error of the mean (SEM) in MTT scatter plots or as percentiles in box charts. Statistical analysis was performed by using SigmaPlot 12 (Systat Software Inc., Chicago, IL, USA). A Shapiro–Wilk normality test, with a $p = 0.05$ rejection value, was used to test normal distribution of data prior to further analysis. All pairwise multiple comparisons were performed by one way ANOVA followed by Holm-Sidak posthoc tests for data with normal distribution or by Kruskal–Wallis analysis of variance on ranks followed by Tukey posthoc tests, in case of failed normality test. Statistical significance was accepted for $p < 0.05$ (*).

Results

To investigate in vitro hemocyte attachment dynamics, hemolymph was withdrawn from the posterior adductor muscle sinus of mussels and directly deposited, without pooling or centrifugation, in small volumes (typically 100 μL) onto uncoated polystyrene culture substrates. Hemolymph was immediately covered with MPSS. This procedure actually prevents hemocyte aggregation. Hoffman modulation contrast (HMC) time-lapse videomicroscopy, at a rate of

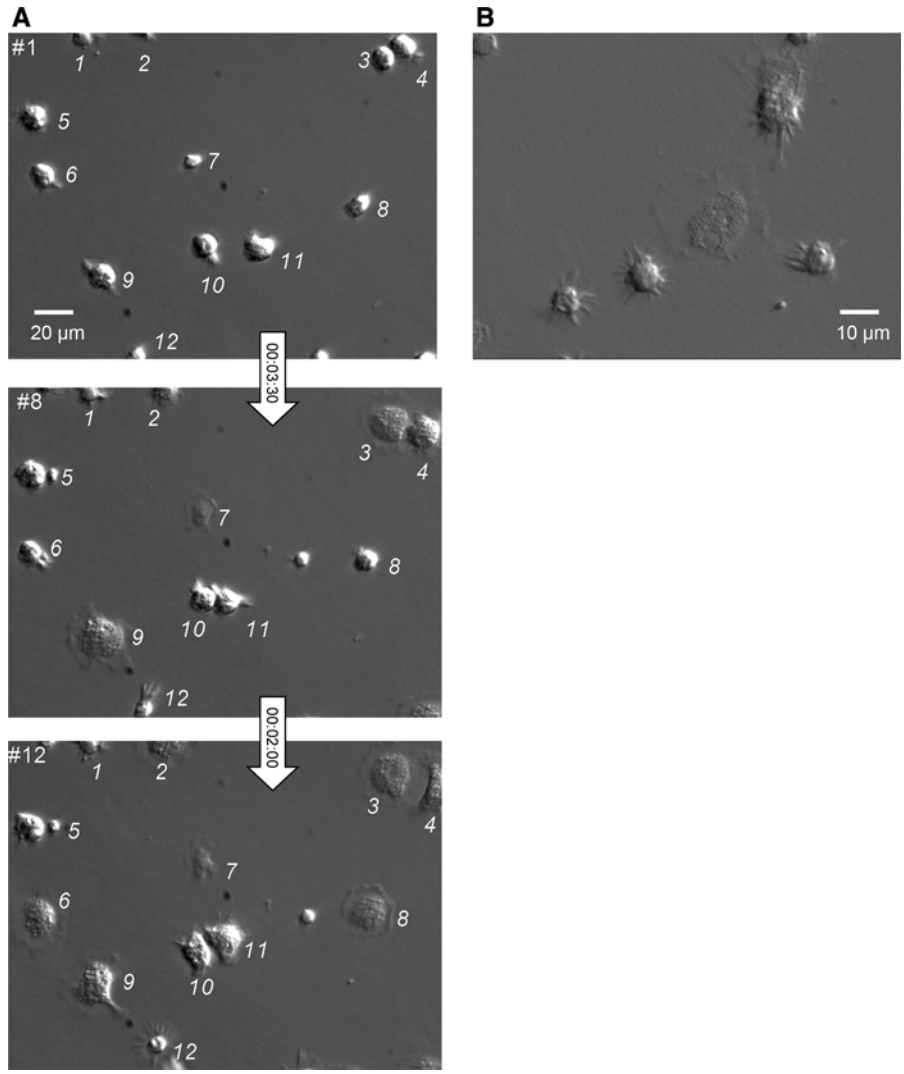

Fig. 1 Hoffman modulation contrast time-lapse imaging of hemocyte attachment in vitro **a** Immediately after withdrawal from the adductor posterior muscle of a single mussel, a droplet of hemolymph was deposited onto a non-treated polystyrene culture dish and covered by MPSS. Cell attachment and movements were monitored by dynamic microscopy at the rate of 1 image every 30 s under ×40 Hoffman modulation contrast magnification. Three of the firsts 12 frames (*numbered in the up-left corner*) corresponding to the same microscopic field are shown. Time intervals are indicated in the arrows (hours:minutes:seconds). To be followed from frame to frame, cells were identified by numbers. Note that most of the cells spread within 5 min (*#3*, *4*, *6*, *7*, *8*, *9*, *10*, *11*) while a small number remained star-shaped (*#1* and *12*). Consult online supplementary video_1 for visualisation of hemocytes in motion. **b** After hemolymph collection as in (**a**), cells were allowed to adhere during 20 min in a polyethyleneimine-coated culture dish. A freeze-frame from a 30-min time-lapse recording is shown, illustrating the main typical shapes of isolated hemocytes, with large spread granular cells distinct from small hemocytes with a round-body surrounded by fast moving filopodia. Video_2 shows that cells kept their shapes during the whole recording

1 image every 30 s, was then carried out to image hemocytes, as shown in Fig. 1a and supplementary video_1. In these conditions, most hemocytes achieved sedimentation and reached the bottom of culture dish within seconds. Following this first step, a majority of round cells changed their shape to adopt a spread outline, revealing a granular cytoplasm and showing amoeboid displacements based on lamellipodia movements. Membrane edges were particularly active as revealed by the presence of numerous transient margin ruffles. Apparently however, some cells were keeping a round body with narrow fast

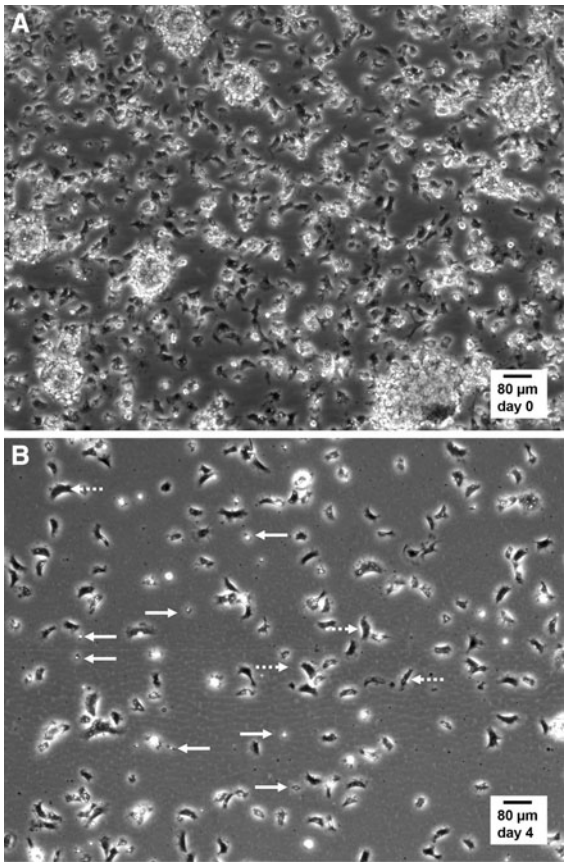

Fig. 2 Still micrographs extracted from live cell time-lapse imaging of mussel hemocytes in culture. Hemocytes in suspension in hemolymph were collected, plated and cultured in MPSS at 14 °C as described in "Materials and methods" section and in Fig. 1. Time-lapse recordings were performed at 14 °C in a Peltier-cooling microscope stage with ×10 phase contrast objective lens. **a** Representative image selected from supplementary video_3 (duration 30 min, 1 image per 30 s), recorded in the droplet of hemolymph, immediately after the initial 20-min phase of adherence and before adding MPSS. Notice the high cell density and the presence of hemocyte aggregates. **b** Representative image selected from supplementary video_4 (duration 30 min, 1 image per 30 s), recorded after 4 days of culture in MPSS. Spread bipolar cells covered large distances by amoeboid movements (*dotted arrows*), while small round star-shaped hemocytes displayed static filopodia protrusions (*solid arrows*)

moving thick filopodia. In order to follow hemocyte shape changes in condition of limited cell displacements, some experiments were repeated on polyethyleneimine-coated culture dishes. This surface treatment promotes cell adhesion (Lelong et al. 1992). In these conditions, morphologic differences between round filopodia-exhibiting cells and spread granulocytes were enhanced (Fig. 1b and supplementary video_2).

In order to characterize hemocyte motility, phase contrast wide field long-term time-lapse recordings (1 image/30 s) were performed at 14 °C under controlled temperature. Typically, after plating, cells were allowed to adhere 20 min and then imaged over 30 min in the drop of hemolymph. In the representative video (supplementary video_3) and the corresponding snapshot (Fig. 2a), the hemocytes appeared to be attached at high density onto the culture substrate, in a mixture of dispersed cells and small sparse aggregates. The cell population was highly motile, with nonstop deformations and random displacements. Hemocytes frequently crossed over each other. After 4 days of culture in marine physiological salt solution (MPSS), the density of hemocytes decreased, mainly because the cells were now distributed on the whole culture surface (11.78 cm^2). Cells were mainly individualized and no aggregate were observed. The two main hemocyte morphologies can be easily distinguished (Fig. 2b and video_4), small star-shaped weakly motile cells (solid arrows) and spread granular cells in fast motion with, for the most part of time, a bipolar bean shape (dashed arrows).

To quantify hemocyte velocity, we had to track simultaneously several motile cells with continuous outline deformations. To simplify the approach, we chose to follow the position of nuclei over time, after vital staining with the DNA fluorescent probe Hoechst 33342. Figure 3a, b shows time-lapse fluorescent images of nuclei obtained at 5 min intervals, with corresponding HMC micrographs at the beginning and at the end of sequences and with superimposed trajectories for the last image (see also supplementary video_5 and video_6). Using this methods, nuclei can be stained immediately before tracking and followed over 30 min. To compare motile activity to cell viability, MTT was used as an indicator of metabolically active mitochondria. However, preliminary results gave great variability in MTT responses immediately after plating. Therefore, we undertook an estimation of repeatability of hemolymph puncture by carrying out MTT bioassays on hemolymph samples collected on a homogeneous pool of 99 mussels and withdrawn by the same operator. Results revealed a wide distribution of MTT OD, with values from 0.05 to 1.05 (Fig. 4a). A Log normal relation can be fitted to the distribution of hemocyte content in hemolymph

samples (histogram binning by 0.05 MTT OD width), only after arbitrary rejection of the first two classes. No other distributions were explored. Despite variability of hemolymph collection, MTT responses increased linearly (slope $9.91 \times 10^{-4} \pm 2.80 \times 10^{-4}$ MTT OD unit/hemolymph µL, $r^2 = 0.9925$) with tested hemolymph volumes (Fig. 4b). This latter result indicates that cell viability can be monitored in cell cultures by using MTT OD relative to values obtained at plating.

Hemocyte velocity determination by nuclei tracking were combined to mitochondria metabolic rate measurements, assessed by MTT bioassays, in order to monitor global cell population activity over 4 days of culture in MPSS at 14 °C. Velocity measurements were performed on a set of 20 hemocytes, selected randomly in the microscopic field after 30 min time-lapse recording, in a separate culture dish for each day of experiment. Cells escaping the recorded field or belonging to aggregates were excluded from the analysis. Four independent culture replicates have been carried out, giving a total of 80 hemocyte velocities per time point. The first day of culture, the mean cell velocity was established at 2.78 ± 0.12 µm min^{-1} ($n = 80$, Fig. 5a). The 5th/95th percentiles, corresponding the 5 % of the population with slowest and fastest migration speeds, show velocities of 0.95 and 4.25 µm min^{-1}, respectively. After 24 h of culture, migration velocities increased transiently and significantly to reach a mean value of 4.56 ± 0.17 µm min^{-1}. This effect was accompanied by a dispersion of speed extrema, with values of 1.45 and 7.10 µm min^{-1} for the 5th and 95th percentiles, respectively. Hemocyte motile activity then declined progressively, to meet initial mean and dispersion at days 3 and 4. Concomitant MTT bioassays revealed a significant peak of metabolic activity at day 2, followed by a decrease of MTT OD below afterwards, with final values (Fig. 5b).

Discussion

In this work, we provide for the first time a quantitative value for mussel hemocyte velocity in vitro, by recording hemocyte cell populations in condition of random walk in free field. The mean initial migration speed, 2.78 µm min^{-1} at 14 °C in MPSS, is similar to velocities reported for human extravascular neutrophils in vivo (2.88 µm min^{-1}) at 37 °C (Kreisel et al. 2010). This reveals that mussel hemocytes can be considered as relatively strong motile cells. Our results also indicate that these cells can be maintained in culture at least 4 days in a basal saline medium, since hemocytes still had similar migration speeds after this period. The temperature of 14 °C was the lowest value achievable by the Peltier-cooled microincubator for continuous imaging under the microscope stage and was therefore also used as set point for the cell culture incubator.

The initial velocity recorded at the onset of culture transiently increased to peak at 4.5 µm min^{-1} (mean populational value) after 24 h, fastest cells exhibiting speeds over 7 µm min^{-1}. This observation could be ascribed to an activation of hemocytes, evocative of an inflammatory response, after withdrawal and plating in the culture environment. This hypothesis is supported by the contemporaneous transient rise of mitochondria metabolic rate revealed by MTT tests. In addition, when deposited in a culture dish, hemocytes collected in suspension in hemolymph immediately attached to the plactic substrate. No cell was observed to remain in suspension. Cell attachment to substrate *per se* may participate to the increase of immune activity and respiratory burst. In mammals, immune cells are known to migrate rapidly towards the site of infection (Abadie et al. 2005; Chtanova et al. 2008; Germain et al. 2012). Interestingly, *ex vivo* explant experiments give evidence for accelerated random migration of immune cells, at rates of 8 µm min^{-1}, similar to interstitial velocities reported for neutrophils at sites of inflammation (Graham et al. 2009; Kreisel et al. 2010). These data are in a good agreement with the highest velocities measured from mussel hemocytes herein. Also in accordance with stimulations of hemocyte motility induced by microbial infections, a recent study reported hemocyte migration within adductor muscle of *Mytilus*

Fig. 3 Determination of cell trajectories and velocities by live cell nuclei tracking. Hemocyte nuclei were specifically stained with Hoechst 33342. Wide field epifluorescence microscopy was used for time-lapse recording of nuclei movements under ×40 magnification. **a** and **b** correspond to distinct recordings (video_5 and video_6), where initial positions of hemocytes in the microscope field are shown in a first Hoffman modulation contrast micrograph (*HMC#1*). Several inverted images of hemocyte nuclei fluorescence at 5 min intervals are shown. A final HMC micrograph is presented at the end of the sequence (*HMC#2*) with different reconstituted nuclei trajectories superimposed ▶

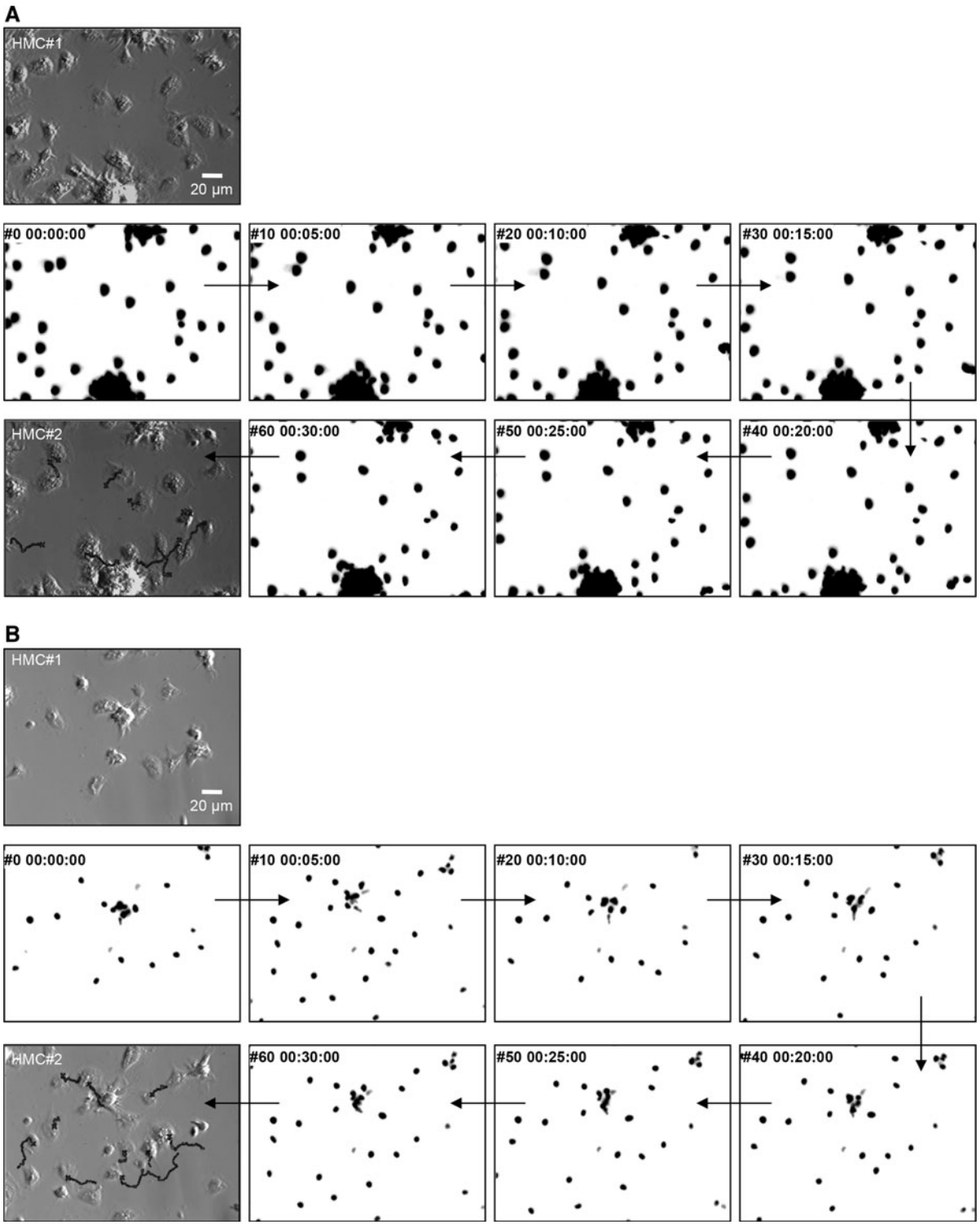

galloprovincialis injected with *Vibrio splendidus* LGP32 (Li et al. 2008). Obviously, these findings lead to include hemocyte migration velocity within the phyiological parameters useful to describe the status of innate immunity in bivalves. In particular, motility monitoring appears to be an excellent indicator of cell

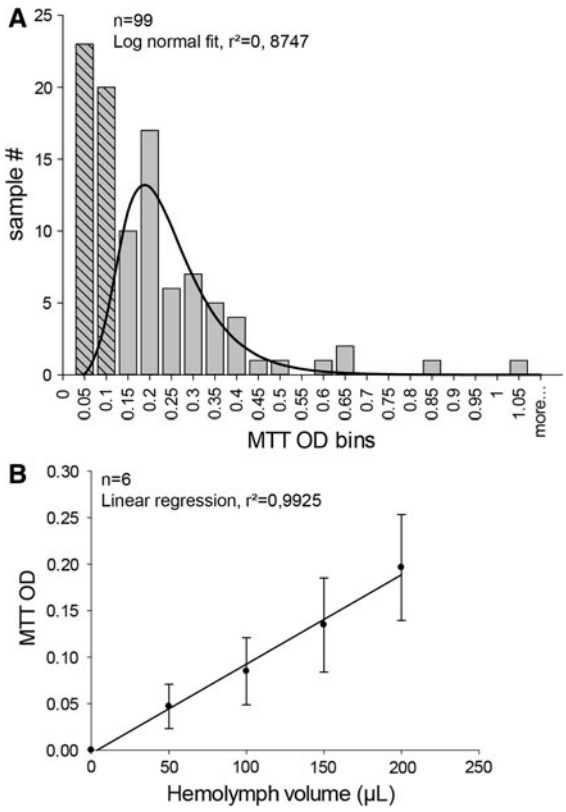

Fig. 4 Assessment of hemocyte content in hemolymph samples by MTT bioassays. **a** To estimate repeatability of hemolymph withdrawal, samples of hemolymph were collected from 99 individual mussels. A volume of 200 µL from each sample was used to determine cell content via MTT bioassays. Resulting optical densities were binned into 22 levels from 0 to 1.05. The first two bins were ignored and the histogram was fitted by a Log normal distribution, giving a peak at OD = 0.22 ± 0.01 ($r^2 = 0.87$). **b** Volumes ranging from 50 to 200 µL of raw hemolymph from 6 mussels were used to measure linearity of MTT responses. Linear regression of mean MTT OD gives a slope of $9.91 \times 10^{-4} \pm 2.80 \times 10^{-4}$ MTT O.D. unit/hemolymph µL with $r^2 = 0.9925$

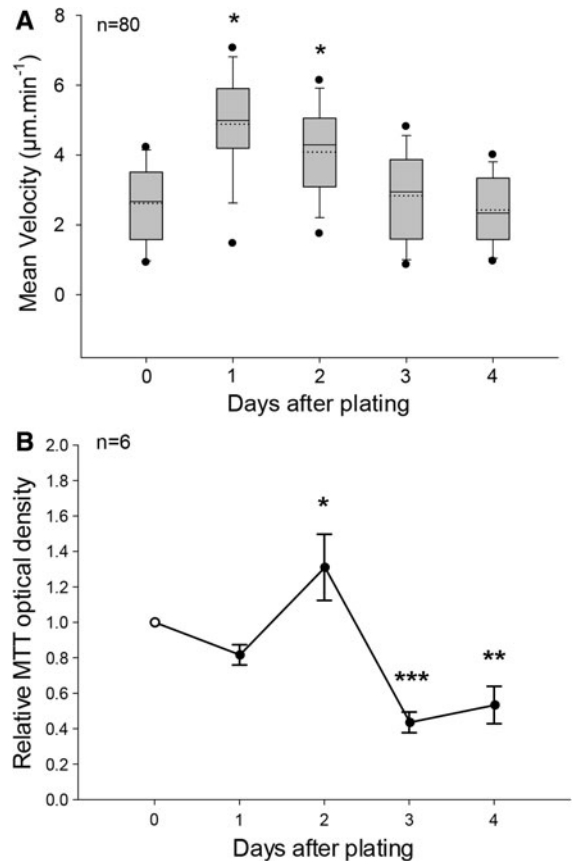

Fig. 5 Evolution of hemocyte velocity and mitochondrial metabolic rate in vitro. **a** Mean velocities were computed from migration distances recorded during 30-min time-lapse nuclei tracking in the culture dish after Hoechst 33342 staining. In 4 replicated cell cultures obtained from individuals, mean cell velocities were determined from 20 trajectories at days 0, 1, 2, 3 and 4 and plotted in a box chart. Box boundaries indicate the 25th (*bottom*) and the 75th (*top*) percentiles. A *solid line* within the box marks the median, and a *dashed line* the mean. Whiskers below and above the box indicate the 10th/90th percentiles. *Outlying points* show the 5th/95th percentiles. Velocities significantly different from value at day 0 are indicated ($*p < 0.05$, Kuskal-Wallis ANOVA on ranks, Tukey post hoc). **b** Changes in MTT responses of cultured hemocytes over time, expressed as a ratio ± SEM (n = 6) relative to seeding values at day 0 (*open circle*). MTT OD significantly different from value at day 0 are indicated ($*p < 0.05$, $**p < 0.01$, $***p < 0.001$, one-way ANOVA, Holm-Sidak post hoc)

activity in culture, in addition to common viability tests such as MTT.

The time-related variations in migration speed of mussel hemocytes in culture indicate that motility is regulated. The dispersion of velocities between slowest and fastest cells, enhanced at the peak of speed, may reflect the presence of distinct cell subpopulations. Given that (1) fluorescent nuclei were randomly selected for cell tracking and (2) hemocytes were capable of fast shape changes, we consider that these differences cannot be definitely attributed to the occurrence of previously characterized less-motile small round basophils and spread eosinophilic granulocytes (Le Foll et al. 2010). Again, fast shape changes associated to hemocyte motion and cell to cell interactions should trigger caution when interpreting morphological variations as makers of effects (Magazine et al. 1996; Hoher et al. 2012). In addition, attention should be drawn to variability of MTT

responses in fresh hemolymph samples. This result can be accounted for by interindividual diffrences in total hemocyte count or in distribution between circulating and infiltrated cells, as already suggested (Cajaraville and Pal 1995; Hoher et al. 2012; Hughes et al. 1991; Li et al. 2008), but also by a poor reproducibility in hemolymph sampling. However, in our experients, MTT OD varied linearly as a function of plated hemolymph volumes. MTT viability bioassays can therefore be used to follow global activity in hemocyte cultures, when expressed relatively to the initial value at plating.

In conclusion, the present work provides a novel approach to investigate hemocyte activity. Our analysis of mussel hemocyte migration highly suggests that motility is very sensitive to cell environmental factors, including cell sampling and/or culturing. Mussel hemocyte migration studies may be of prime pathophysiological significance since two independent transcriptomic studies have identified a conserved cytokine involved in innate immunocyte migration control, the macrophage migration inhibitory factor (MIF), as a major immune-related transcript (Philipp et al. 2012; Venier et al. 2011). The method described herein could be used in further investigations aiming at characterizing hemocyte motility in response to seasonal variations, environment changes, bacterial challenges and chemoattractants.

Acknowledgments This work was supported by grants from the State/Region Plan Contract (CPER) allocated through the Research Federation FED 4116 SCALE (Sciences Appliquées à L'Environnement). Damien Rioult were recipients for doctoral fellowships from the Conseil Regional de Haute-Normandie.

References

Abadie V, Badell E, Douillard P, Ensergueix D, Leenen PJ, Tanguy M, Fiette L, Saeland S, Gicquel B, Winter N (2005) Neutrophils rapidly migrate via lymphatics after Mycobacterium bovis BCG intradermal vaccination and shuttle live bacilli to the draining lymph nodes. Blood 106:1843–1850. doi:10.1182/blood-2005-03-1281

Cajaraville MP, Pal SG (1995) Morphofunctional study of the haemocytes of the bivalve mollusc *Mytilus galloprovincialis* with emphasis on the endolysosomal compartment. Cell Struct Funct 20:355–367

Carballal MJ, Lopez C, Azevedo C, Villalba A (1997) Enzymes involved in defense functions of hemocytes of mussel *Mytilus galloprovincialis*. J Invertebr Pathol 70:96–105

Chtanova T, Schaeffer M, Han SJ, van Dooren GG, Nollmann M, Herzmark P, Chan SW, Satija H, Camfield K, Aaron H, Striepen B, Robey EA (2008) Dynamics of neutrophil migration in lymph nodes during infection. Immunity 29:487–496. doi:10.1016/j.immuni.2008.07.012

Costa MM, Prado-Alvarez M, Gestal C, Li H, Roch P, Novoa B, Figueras A (2009) Functional and molecular immune response of Mediterranean mussel (*Mytilus galloprovincialis*) haemocytes against pathogen-associated molecular patterns and bacteria. Fish Shellfish Immunol 26:515–523

Craft JA, Gilbert JA, Temperton B, Dempsey KE, Ashelford K, Tiwari B, Hutchinson TH, Chipman JK (2010) Pyrosequencing of *Mytilus galloprovincialis* cDNAs: tissue-specific expression patterns. PLoS ONE 5:e8875. doi:10.1371/journal.pone.0008875

Donaghy L, Volety AK (2011) Functional and metabolic characterization of hemocytes of the green mussel, Perna viridis: in vitro impacts of temperature. Fish Shellfish Immunol 31:808–814

Friebel B, Renwrantz L (1995) Application of density gradient centrifugation for separation of eosinophilic and basophilic hemocytes from *Mytilus edulis* and characterization of both cell groups. Comp Biochem Physiol A Mol Integr Physiol 112A:81–90

Garcia-Garcia E, Prado-Alvarez M, Novoa B, Figueras A, Rosales C (2008) Immune responses of mussel hemocyte subpopulations are differentially regulated by enzymes of the PI 3-K, PKC, and ERK kinase families. Dev Comp Immunol 32:637–653

Gauthier-Clerc S, Boily I, Fournier M, Lemarchand K (2013) In vivo exposure of *Mytilus edulis* to living enteric bacteria: a threat for immune competency? Environ Sci Pollut Res Int 20(2):612–620. doi:10.1007/s11356-012-1200-x

Germain RN, Robey EA, Cahalan MD (2012) A decade of imaging cellular motility and interaction dynamics in the immune system. Science 336:1676–1681. doi:10.1126/science.1221063

Graham DB, Zinselmeyer BH, Mascarenhas F, Delgado R, Miller MJ, Swat W (2009) ITAM signaling by Vav family Rho guanine nucleotide exchange factors regulates interstitial transit rates of neutrophils in vivo. PLoS ONE 4:e4652. doi:10.1371/journal.pone.0004652

Hine P (1999) The inter-relationships of bivalve haemocytes. Fish Shellfish Immunol 9:367–385

Hoher N, Kohler A, Strand J, Broeg K (2012) Effects of various pollutant mixtures on immune responses of the blue mussel (*Mytilus edulis*) collected at a salinity gradient in Danish coastal waters. Mar Environ Res 75:35–44. doi:10.1016/j.marenvres.2011.11.003

Hughes TK Jr, Smith EM, Barnett JA, Charles R, Stefano GB (1991) Lipopolysaccharide and opioids activate distinct populations of *Mytilus edulis* immunocytes. Cell Tissue Res 264:317–320

Kreisel D, Nava RG, Li W, Zinselmeyer BH, Wang B, Lai J, Pless R, Gelman AE, Krupnick AS, Miller MJ (2010) In vivo two-photon imaging reveals monocyte-dependent neutrophil extravasation during pulmonary inflammation. Proc Natl Acad Sci USA 107:18073–18078. doi:10.1073/pnas.1008737107

Le Foll F, Rioult D, Boussa S, Pasquier J, Dagher Z, Leboulenger F (2010) Characterisation of *Mytilus edulis*

hemocyte subpopulations by single cell time-lapse motility imaging. Fish Shellfish Immunol 28:372–386. doi: 10.1016/j.fsi.2009.11.011

Lelong IH, Petegnief V, Rebel G (1992) Neuronal cells mature faster on polyethyleneimine coated plates than on polylysine coated plates. J Neurosci Res 32:562–568. doi: 10.1002/jnr.490320411

Li H, Parisi MG, Toubiana M, Cammarata M, Roch P (2008) Lysozyme gene expression and hemocyte behaviour in the Mediterranean mussel, *Mytilus galloprovincialis*, after injection of various bacteria or temperature stresses. Fish Shellfish Immunol 25:143–152

Magazine HI, Liu Y, Bilfinger TV, Fricchione GL, Stefano GB (1996) Morphine-induced conformational changes in human monocytes, granulocytes, and endothelial cells and in invertebrate immunocytes and microglia are mediated by nitric oxide. J Immunol 156(12):4845–4850

Malagoli D, Casarini L, Sacchi S, Ottaviani E (2007) Stress and immune response in the mussel *Mytilus galloprovincialis*. Fish Shellfish Immunol 23:171–177

Novas A, Barcia R, Ramos-Martinez JI (2007) Nitric oxide production by haemocytes from *Mytilus galloprovincialis* shows seasonal variations. Fish Shellfish Immunol 23:886–891

Parisi MG, Li H, Jouvet LB, Dyrynda EA, Parrinello N, Cammarata M, Roch P (2008) Differential involvement of mussel hemocyte sub-populations in the clearance of bacteria. Fish Shellfish Immunol 25:834–840

Philipp EE, Kraemer L, Melzner F, Poustka AJ, Thieme S, Findeisen U, Schreiber S, Rosenstiel P (2012) Massively parallel RNA sequencing identifies a complex immune gene repertoire in the lophotrochozoan *Mytilus edulis*. PLoS ONE 7:e33091. doi:10.1371/journal.pone.0033091

Ponder W, Lindberg D (2008) Chap. 1. In: Ponder W, Lindberg D (Eds.) Phylogeny and evolution of Mollusca, University of Calfornia Press, pp 1–18

Venier P, Varotto L, Rosani U, Millino C, Celegato B, Bernante F, Lanfranchi G, Novoa B, Roch P, Figueras A, Pallavicini A (2011) Insights into the innate immunity of the Mediterranean mussel *Mytilus galloprovincialis*. BMC Genomics 12:69

Voccia I, Krzystyniak K, Dunier M, Flipo D, Fournier M (1994) In vitro mercury-related cytotoxicity and functional impairment of the immune cells of rainbow trout (*Oncorhynchus mykiss*). Aquat Toxicol 29:37–48

Winston GW, Moore MN, Kirchin MA, Soverchia C (1996) Production of reactive oxygen species by hemocytes from the marine mussel, *Mytilus edulis*: lysosomal localization and effect of xenobiotics. Comp Biochem Physiol C Pharmacol Toxicol Endocrinol 113:221–229

Zhang G, Fang X, Guo X, Li L, Luo R, Xu F, Yang P, Zhang L, Wang X, Qi H, Xiong Z, Que H, Xie Y, Holland PW, Paps J, Zhu Y, Wu F, Chen Y, Wang J, Peng C, Meng J, Yang L, Liu J, Wen B, Zhang N, Huang Z, Zhu Q, Feng Y, Mount A, Hedgecock D, Xu Z, Liu Y, Domazet-Loso T, Du Y, Sun X, Zhang S, Liu B, Cheng P, Jiang X, Li J, Fan D, Wang W, Fu W, Wang T, Wang B, Zhang J, Peng Z, Li Y, Li N, Chen M, He Y, Tan F, Song X, Zheng Q, Huang R, Yang H, Du X, Chen L, Yang M, Gaffney PM, Wang S, Luo L, She Z, Ming Y, Huang W, Huang B, Zhang Y, Qu T, Ni P, Miao G, Wang Q, Steinberg CE, Wang H, Qian L, Liu X, Yin Y (2012) The oyster genome reveals stress adaptation and complexity of shell formation. Nature 490:49–54. doi:10.1038/nature11413